Supporting Information

Tailored PolyMOFs for Ion Transport in Lithium-based Battery Electrolyte

Ian J. Dillingham,[1] Vibhu Vardhan Singh[2,3], Rebecca Y. Han,[1] Liwen F. Wan[3,4*], and V. Sara Thoi[1,5*]

[1] Department of Chemistry, Johns Hopkins University, Baltimore, Maryland 21218, USA.
[2] Aiiso Yunfeng Li Family of Chemical and Nano Engineering, University of California San Diego, 9500 Gilman Drive La Jolla, CA 92093, USA.
[3] Materials Science Division, Lawrence Livermore National Laboratory, Livermore, California 94550 USA.
[4] Laboratory for Energy Applications for the Future, Lawrence Livermore National Laboratory, Livermore, California 94550 USA
[5] Department of Materials Science and Engineering, Johns Hopkins University, Baltimore, Maryland 21218, USA.

*Corresponding authors: sarathoi@jhu.edu, wan6@llnl.gov

Table of Contents

Figures and Tables

Figure S1. Electrochemical impedance spectroscopy cell setup. Kapton-covered vise sandwiches two copper strips and the EIS pellet cell (sealed with electrical tape) to retain contact and constant pressure.

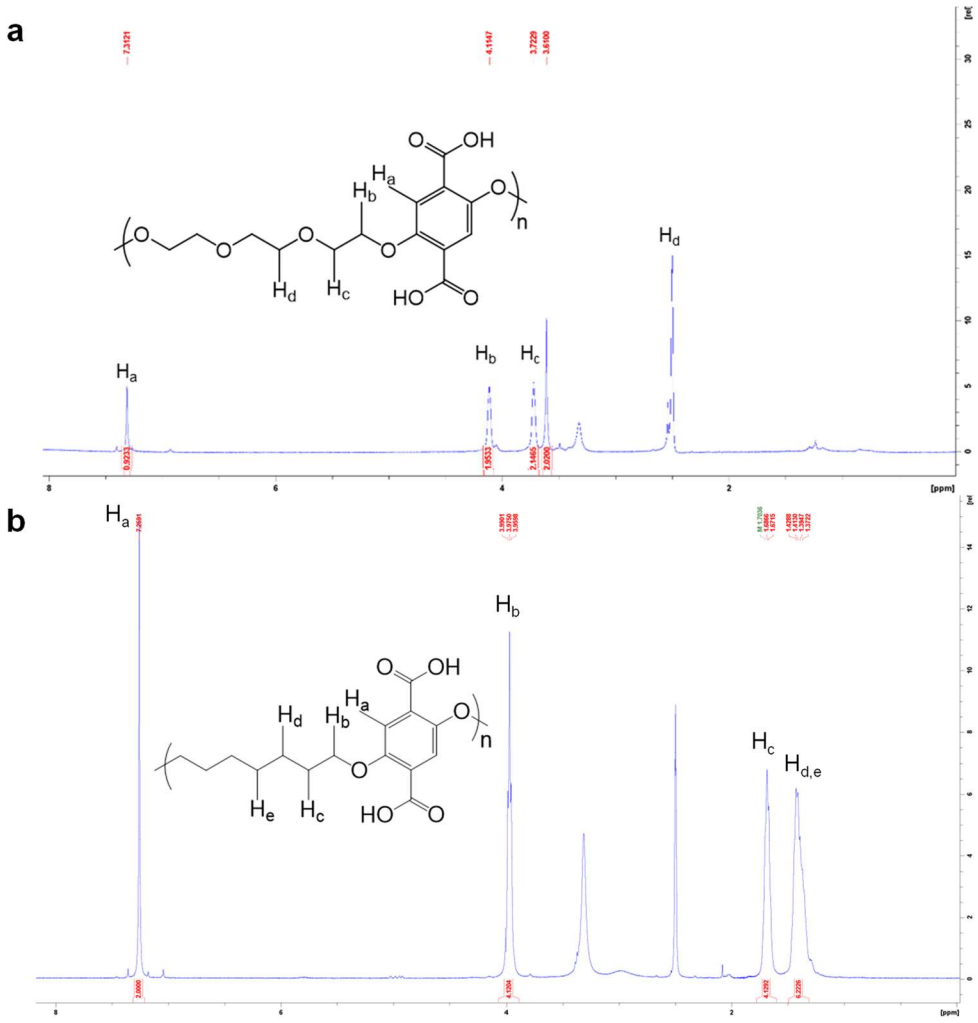

Figure S2. ^{1}H NMR of pbdc-8peg (a) and pbcd-7pe (b) with associated chemical structures and proton assignments

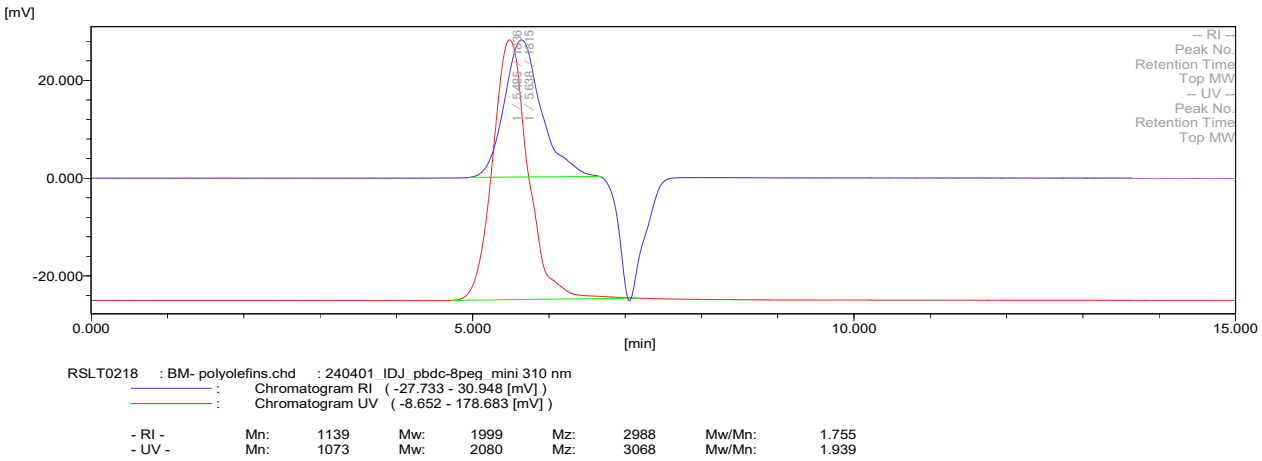

Figure S3. Gel permeation chromatography trace of pbdc-8peg, the polylinker used to synthesize polyUiO-66-PEG. Molecular weight values for both refractive index (RI) and ultraviolet (UV) detectors is shown at the bottom.

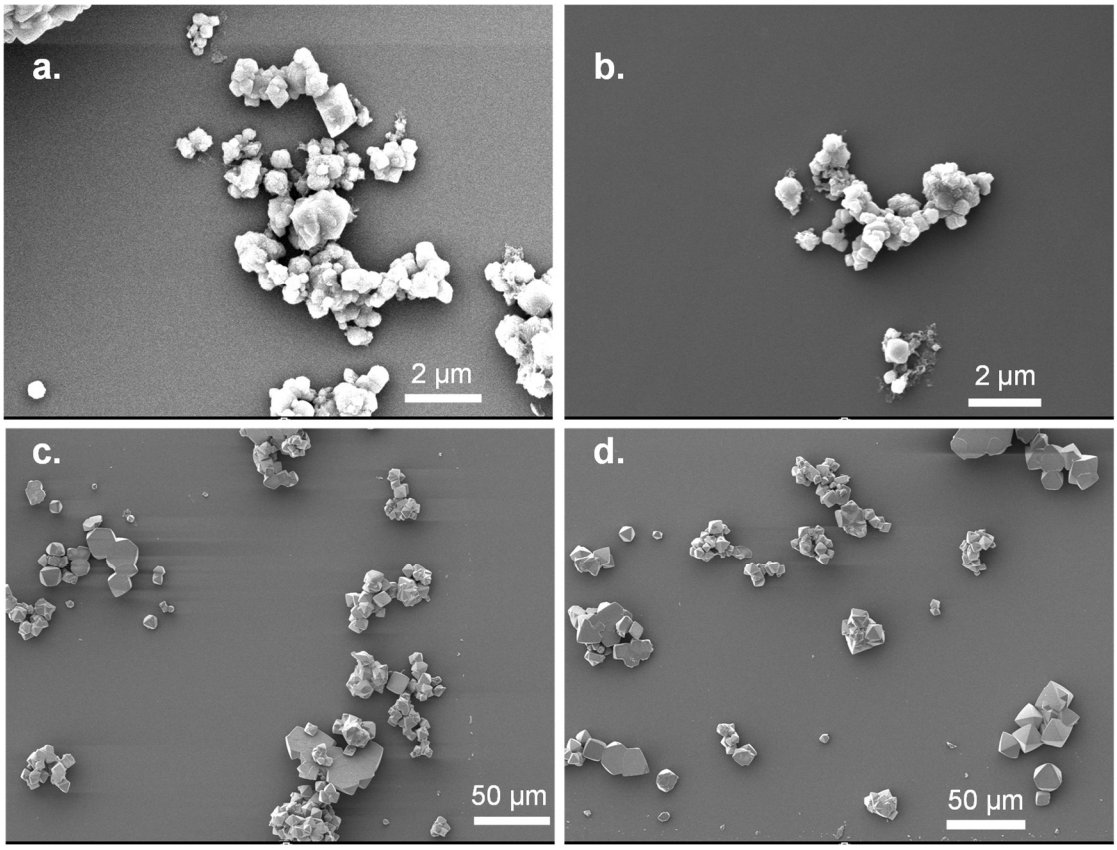

Figure S4. Scanning electron microscope imagery of (a,b) polyUiO-66-PE and (c,d) polyUiO-66-PEG particles

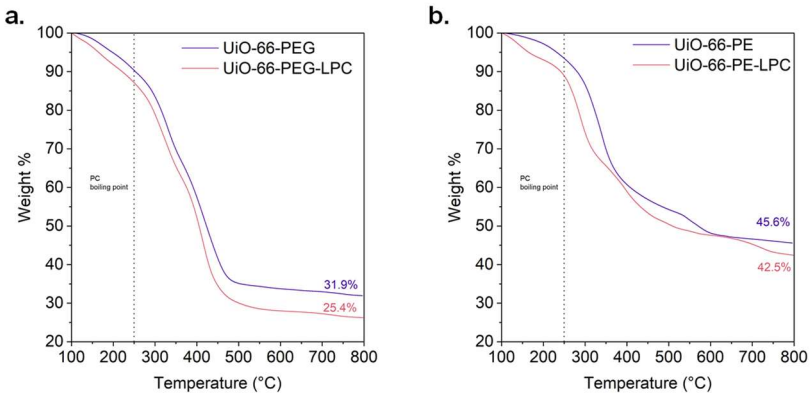

Figure S5. TGA of polyUiO-66-PEG and polyUiO-66-PE after isothermal heating at 100 °C for 60 min to remove residual physisorbed solvents. Each sample was run before and after soaking with 1.0 M LiClO4 in PC electrolyte solution, with the boiling point of PC denoted.

Table S1. Molar ratio of MOF to Li of dried polyMOF powders after soaking in 1.0 M $LiClO_4$/PC solution.

$LiClO_4$/PC-soaked MOF sample	Molar MOF:Li ratio*
polyUiO-66-PE	1 : 9.39
polyUiO-66-PEG	1 : 9.45

*Li content was determined using AAS, with samples completely digested in H_2SO_4 for 12 h before dilution with DI water and using a standard calibration curve.

Method for PC quantification in MOF samples. PC quantification was conducted using a method adapted from literature.[1] Using thermogravimetric analysis, we assume the final mass of the electrolyte-soaked MOF TGA to be composed entirely of ZrO_2 and LiCl (the assumed decomposition products of the metals in the sample. With the calculated ratio of MOF repeating unit to Li from AAS (**Table S1**), we calculate the quantity of PC in the initial sample of soaked MOF. An example calculation for polyUiO-66-PEG (**Figure S5a)** is shown below:

$$\frac{25.4\%}{(6 \times MW_{ZrO_2} + 9.45 \times MW_{LiCl})} = \frac{100\%}{(MW_{polyUiO-66-PE} + 9.45 \times MW_{LiClO_4} + Z \times MW_{PC})}$$

where the empirical formula of polyUiO-66-PEG is $Zr_6O_4(OH)_4$(pbdc-8peg)$_6$ and MW is the molecular weight. Solving for *Z*, we get 8.27 PC per repeating unit of polyUiO-66-PEG

$$t_{\mathrm{Li+}} = \frac{I_{ss}(\Delta V - I_0 R_0)}{I_0(\Delta V - I_{ss} R_{ss})} \quad \text{(Eq. S1)}$$

Equation S1: Equation for Li^+ transference number, where I_0 and I_{SS} are the initial and steady-state currents, respectively, at either end of the polarization process, ΔV is the magnitude of the applied voltage, and R_0 and R_{ss} are the resistances collected from EIS measurements directly before and after polarization, respectively.[2]

$$\sigma_T = Ae^{\left(\frac{-E_a}{kT}\right)} \quad \text{(Eq. S2)}$$

Equation S2: Arrhenius equation for activation energy of long-range ionic conductivity. σ_T is ionic conductivity at a given temperature, T is temperature in K, E_a is activation energy in eV, and k is the Boltzmann constant.

$$\ln\left(\frac{1}{w} - \frac{1}{A}\right) = -\left(\frac{E_a}{kT}\right) - \ln\left(\frac{1}{B} - \frac{1}{A}\right) \quad \text{(Eq. S3)}$$

Equation S3: Linearized form of Hendrickson and Bray equation, where w is the width of the peak at half-maximum intensity, A is the width of the peak at or below the temperature at which broadening reaches its maximum, and B is the width of the peak at or above the temperature at which broadening reaches its minimum. E_a, k, and T are activation energy of local Li hopping, Boltzmann constant, and temperature in K, respectively

$$\sigma = \frac{l}{R * A} \quad \text{(Eq. 4)}$$

Equation S4: Equation for ionic conductivity from resistance measurements, where σ is ionic conductivity in S cm^{-1}, l is thickness of pellet in cm, A is area of pellet face in cm^2, and R is resistance in Ω.[3]

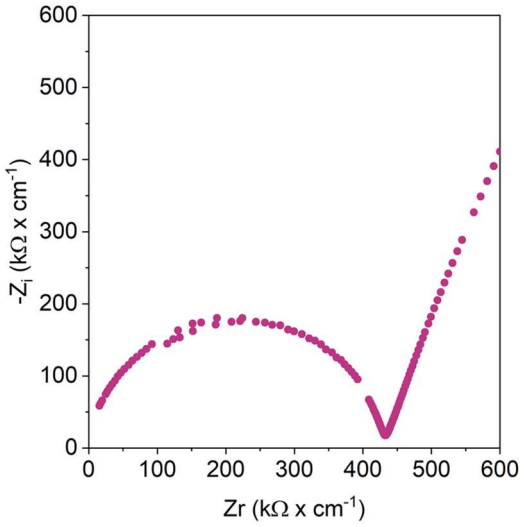

Figure S6. Room temperature (25 ℃) EIS spectrum for UiO-66 loaded with 1.0M $LiClO_4$ in propylene carbonate.

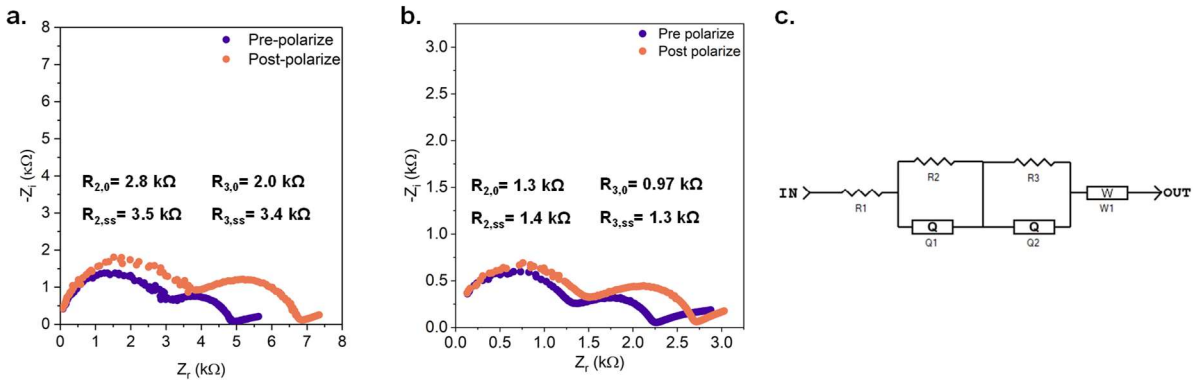

Figure S7. EIS of (a) polyUiO-66-PEG and (b) polyUiO-66-PE before and after polarization using nonblocking Li metal electrodes for Li^+ transference number measurements. (c) equivalent circuit model used for fitting EIS data. Impedance values for (a) and (b) before and after polarization are denoted with subscript "0" and "ss", respectively.

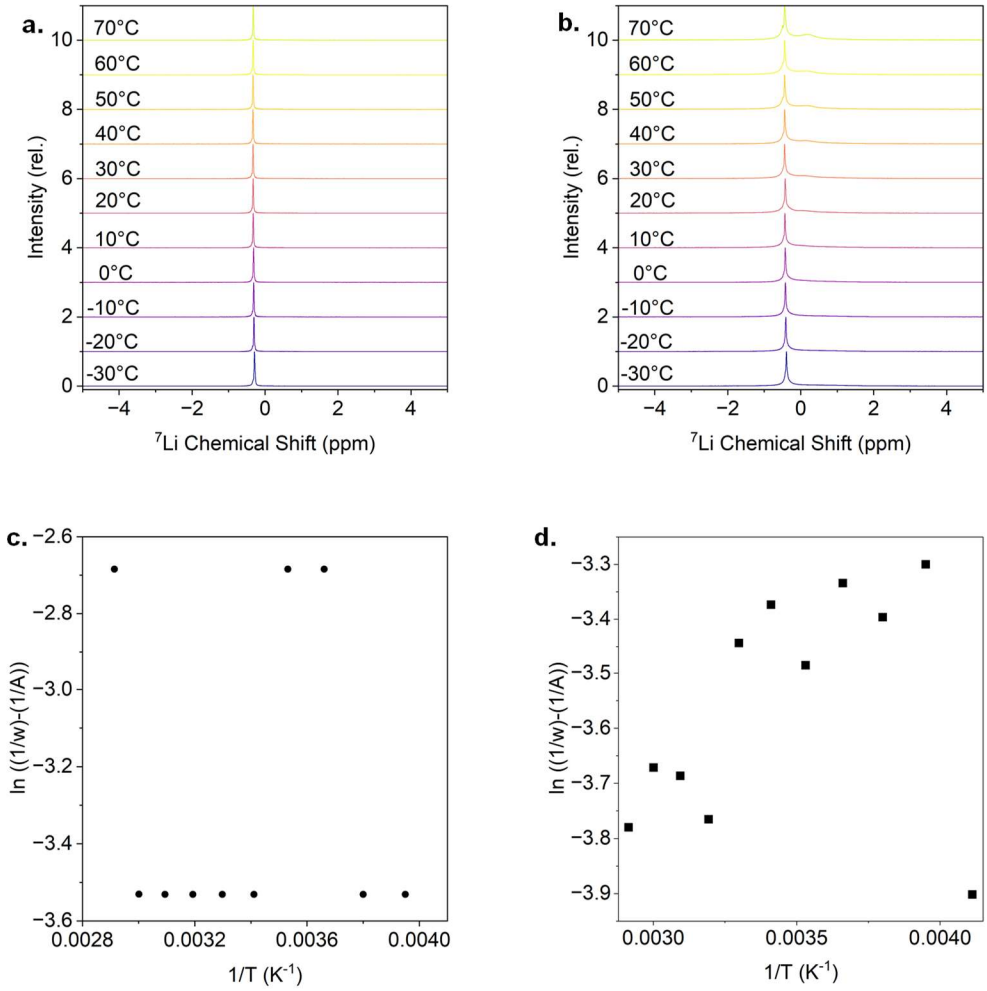

Figure S8. Temperature dependent ^{7}Li solid-state NMR for (a) polyUiO-66-PE, and (b) UiO-66 samples after soaking the samples in 1.0 M $LiClO_4$ in propylene carbonate, with data fit to the Hendrickson and Bray equation showing no linear correlation ((c) is data from polyUiO-66-PE, and (d) is data from UiO-66, using only the main peak width).

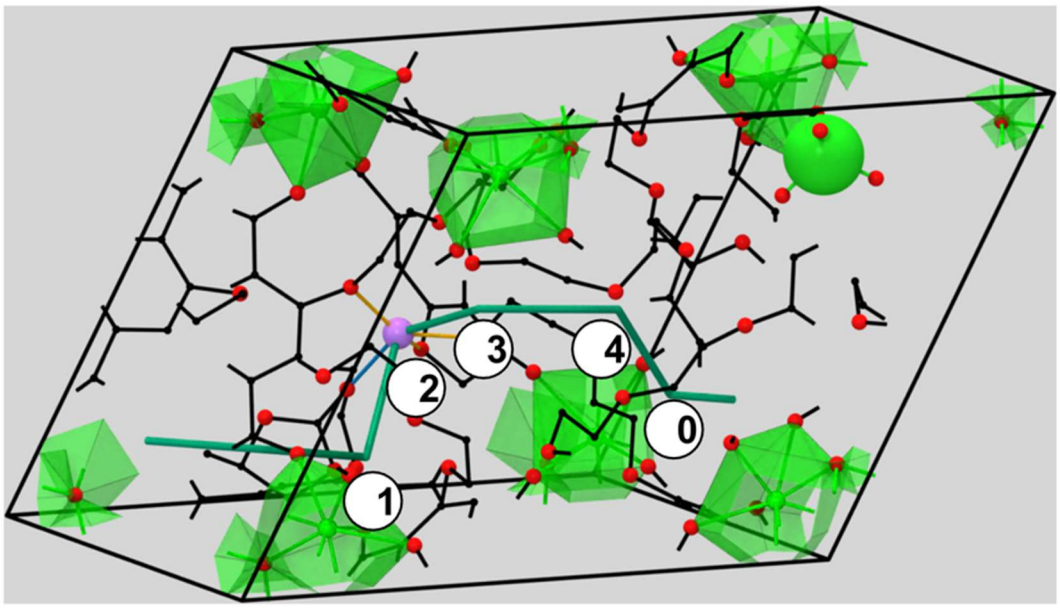

Figure S9. Schematic of different sites across the polyUiO-66-PEG forming a connected pathway

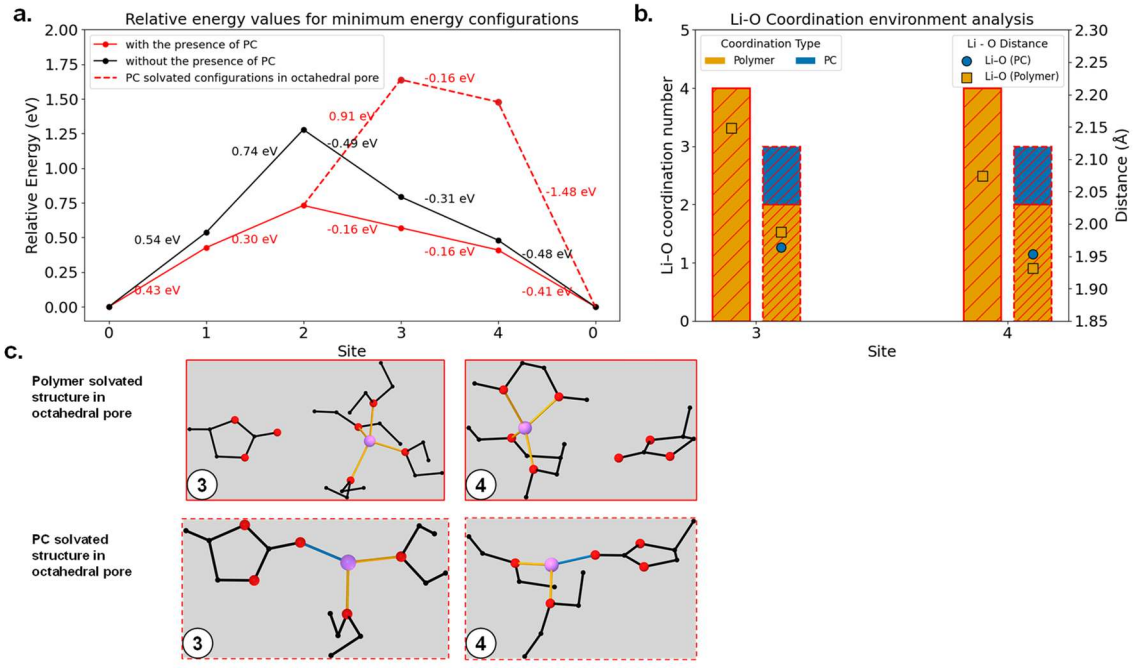

Figure S10. (a) Relative energetics for most stable Li+ configurations at different sites in polyUiO-66-PEG shown with and without the presence of PC in addition to configurations where PC is inside the octahedral void solvating the Li+. (b) Corresponding Li-O coordination number and distance resolved with corresponding solvating species for sites 3 and 4 in the presence of PC. The plot color in (a) corresponds to the bar plot border color in (b). (c) Schematic of minimum energy configurations at site 3 and 4 in the presence of PC. The Li-O bond color is consistent with Li-O coordination number in part (b)

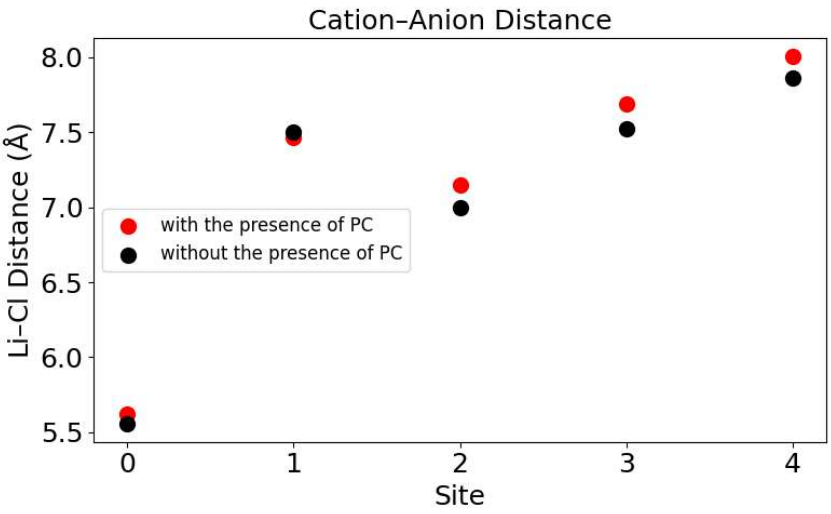

Figure S11. Cation – Anion distance for different sites in polyUiO-66-PEG during the DFT calculations shown with and without the presence of PC

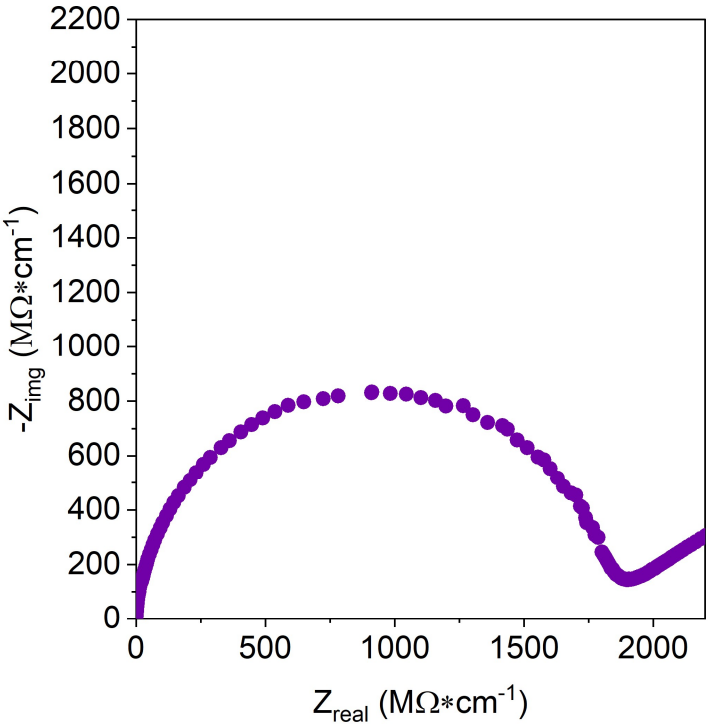

Figure S12. EIS of polyUiO-66-PEG after infiltration with 1.0 M LiTFSI in a 1:1 by volume of DOL:DME solution.

Table S2. Select MOF-based electrolytes in literature.

Electrolyte composition	Type	Ionic conductivity (S cm^{-1})	Li^+ transference number	Ref.
20 wt% ZIF-8, PEO, LiTFSI	MOF-Polymer Composite	2.2×10^{-5} at 30℃	0.36	[4]
10 wt% MIL-53-Al, PEO, LiTFSI	MOF-Polymer Composite	3.9×10^{-3} at 120℃	0.343	[5]
40 wt% UiO-66, PEO, LiTFSI	MOF-Polymer Composite	1.3×10^{-4} at 30℃	0.35	[6]
50 wt% UiO-66, PC/dimethyl carbonate, $LiClO_4$, PVDF-HFP	MOF-polymer Composite	1.5×10^{-4} at room temperature	0.61	[7]
UiO-67, $LiClO_4$, PC	Embedded Electrolyte	6.5×10^{-4} at room temperature	0.65 (for MOF-PTFE composite membrane)	[1]
UiO-66, LiTFSI, [EMIM][TFSI] ionic liquid	Embedded Ionic Liquid	3.2×10^{-4} at 25℃	0.33	[8]
polyUiO-66-PE, $LiClO_4$, PC	**Embedded Electrolyte**	**$6.4 \times 10^{-5} - 3.0 \times 10^{-5}$ at 25℃****	**0.44**	**This work**
polyUiO-66-PEG, $LiClO_4$, PC	**Embedded Electrolyte**	**$1.8 \times 10^{-4} - 7.2 \times 10^{-5}$ at 25℃****	**0.81**	**This work**

PEO = polyethylene oxide (also known as polyethylene glycol, PEG); PVDF-HFP = poly(vinylidene fluoride-co-hexafluoropropylene); EMIM = 1-ethyl-3-methylimidazolium
**intra-grain and total ion conductivity, respectively

References

(1) Shen, L.; Wu, H. B.; Liu, F.; Brosmer, J. L.; Shen, G.; Wang, X.; Zink, J. I.; Xiao, Q.; Cai, M.; Wang, G.; Lu, Y.; Dunn, B. Creating Lithium-Ion Electrolytes with Biomimetic Ionic Channels in Metal–Organic Frameworks. *Advanced Materials* **2018**, *30* (23), 1707476. https://doi.org/10.1002/adma.201707476.

(2) Evans, J.; Vincent, C. A.; Bruce, P. G. Electrochemical Measurement of Transference Numbers in Polymer Electrolytes. *Polymer* **1987**, *28* (13), 2324–2328. https://doi.org/10.1016/0032-3861(87)90394-6.

(3) Vadhva, P.; Hu, J.; Johnson, M. J.; Stocker, R.; Braglia, M.; Brett, D. J. L.; Rettie, A. J. E. Electrochemical Impedance Spectroscopy for All-Solid-State Batteries: Theory, Methods and Future Outlook. *ChemElectroChem* **2021**, *8* (11), 1930–1947. https://doi.org/10.1002/celc.202100108.

(4) Lei, Z.; Shen, J.; Zhang, W.; Wang, Q.; Wang, J.; Deng, Y.; Wang, C. Exploring Porous Zeolitic Imidazolate Frame Work-8 (ZIF-8) as an Efficient Filler for High-Performance Poly(Ethyleneoxide)-Based Solid Polymer Electrolytes. *Nano Res.* **2020**, *13* (8), 2259–2267. https://doi.org/10.1007/s12274-020-2845-2.
(5) Zhu, K.; Liu, Y.; Liu, J. A Fast Charging/Discharging All-Solid-State Lithium Ion Battery Based on PEO-MIL-53(Al)-LiTFSI Thin Film Electrolyte. *RSC Adv.* **2014**, *4* (80), 42278–42284. https://doi.org/10.1039/C4RA06208F.
(6) Wu, J.-F.; Guo, X. MOF-Derived Nanoporous Multifunctional Fillers Enhancing the Performances of Polymer Electrolytes for Solid-State Lithium Batteries. *J. Mater. Chem. A* **2019**, *7* (6), 2653–2659. https://doi.org/10.1039/C8TA10124H.
(7) Lu, X.; Wu, H.; Kong, D.; Li, X.; Shen, L.; Lu, Y. Facilitating Lithium-Ion Conduction in Gel Polymer Electrolyte by Metal-Organic Frameworks. *ACS Materials Lett.* **2020**, *2* (11), 1435–1441. https://doi.org/10.1021/acsmaterialslett.0c00293.
(8) Wu, J.-F.; Guo, X. Nanostructured Metal–Organic Framework (MOF)-Derived Solid Electrolytes Realizing Fast Lithium Ion Transportation Kinetics in Solid-State Batteries. *Small* **2019**, *15* (5), 1804413. https://doi.org/10.1002/smll.201804413.